1-1-1982

The application of the method of pseudocharacteristics to the numerical dynamic simulation of a one dimensional magnetohydrodynamic channel.

Yi-Zun Wang

THE APPLICATION OF THE METHOD OF PSEUDOCHARACTERISTICS TO THE NUMERICAL DYNAMIC SIMULATION OF A ONE DIMENSIONAL MAGNETOHYDRODYNAMIC CHANNEL

by

Yi-Zun Wang

A Thesis

Presented to the Graduate Committee

of Lehigh University

in Candidacy for the Degree of

Master of Science

in

Mechanical Engineering and Mechanics

Lehigh University

1982

Certificate of Approval

This thesis is accepted and approved in partial fulfillment of the requirements for the degree of Master of Science.

Dec 9, 1982
(date)

Professor in Charge

Chairman of Department

Table of contents

List of Tables

List of Figures

Acknowledgment

The author wishes to express her sincere gratitude and appreciation to:

Professor S.H. Johnson for his advice and encouragement in both this work and during her studies at Lehigh,

Professor W.E. Schiesser of Chemical Engineering for his kind help in this work, and

especially, the government of the People's Republic of China for making possible her studies in the United States.

ABSTRACT

An analytical model of one dimensional flow in the channel section of a gasified-coal, magnetohydrodynamic, electric power generator is a set of hyperbolic partial differential equations. It consists of three coupled, nonlinear, first-order partial differential equations in local balance equation form with nonzero production/absorption terms.

Conventional application of the Method of Lines to n fixed, discrete points, uniformly distributed along the channel, produces 3n coupled, temporal, nonlinear, first-order ordinary differential equations. The numerical results for the dynamic simulation of the MHD model show, if a centered finite difference formula is used to replace the spatial derivatives, are numerically stable but severely distorted. If biased formulas are used, the solutions are numerically unstable.

Application of the method of Pseudocharacteristics produces stable solutions but increases the system stiffness. The Pseudocharacteristic equations for the time derivative terms can be obtained either by solving the linear system without matrix inversion or by matrix transformation without solving the linear system.

The Jacobian maps and the eigenvalues of the Jacobian matrices show the system stiffness and stability.

1. MHD Channel Model

The mathematical formulation of the transient processes in large magnetohydrodynamic generator flow trains was described by Oliver, Crouse, Maxwell and Demetriades [2]. In that paper, the flow trains were assumed to consist of a combustor, nozzle, magnetohydrodynamic power generation channel and a diffuser. For the purpose of this study, only the channel section is considered.

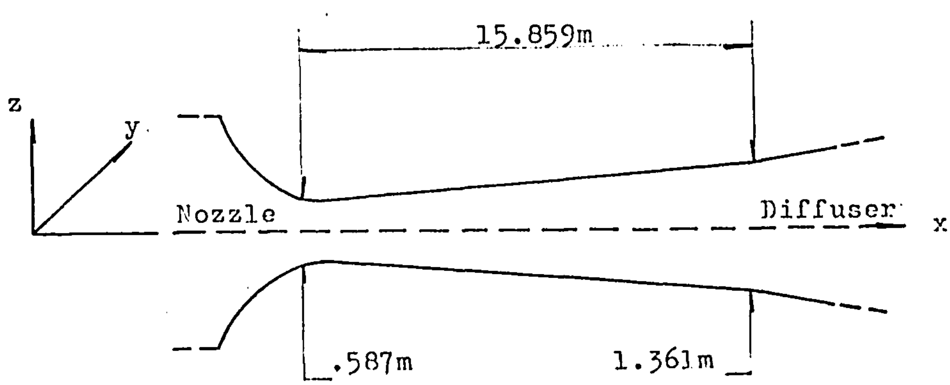

Figure 1. Dimensions of a Hypothetical Channel

As shown in Figure 1, x is the axial coordinate in the flow direction, y, z are cross-sectional coordinates. z is aligned with the magnetic field. Time is denoted by t. For homogeneous flow, the element mass fraction equation (1) in [2] is ignored. The conservation laws in the quasi-one-dimensional approximate model yield:

conservation of total mass equation

$$\frac{\partial}{\partial t}(\rho A) + \frac{\partial}{\partial x}(\rho UA) = S_\rho \quad , \tag{1}$$

conservation of linear momentum equation

$$\frac{\partial}{\partial t}(\rho UA) + \frac{\partial}{\partial x}(\rho U^2 A) = -A\left(\frac{\partial p}{\partial x} - \langle J \times B \rangle_x\right) - \tau_w P + S_u \quad , \tag{2}$$

and conservation of energy equation

$$\frac{\partial}{\partial t}[\rho(\varepsilon + U^2)A] + \frac{\partial}{\partial x}(\rho U h_o A) = \langle J . E \rangle_x A + q_w P + S_\varepsilon \quad . \tag{3}$$

The terms S_ρ, S_u, S_ε are functions describing the sources of mass, momentum and energy due to mass addition and absorption within the flow train. They are determined by the mass injection locations within the various sections of the flow train, particularly for the combustor, so these three terms are neglected in the channel section model.

Also, assuming the fluid behaves like an ideal gas, $p = RT\rho$. The average shear stress over the cross-section $\tau_w \sim 0$, and the average heat flux $q_w \sim q_{rad}$.

The radative flux q_{rad} is represented as

$$q_{rad} = \sigma_{sb}(\varepsilon_w T_w^4 - \varepsilon_g T^4),$$

thermodynamic relations are

Stagnation enthalpy $h_o = h + U^2/2$

internal energy $\varepsilon = h - p/\rho$, The local electric field and current density within the cross-section of the duct at any axial station x are $\underline{E}(x,y,z,t)$ and $\underline{J}(x,y,z,t)$.

Lorentz force in the axial direction

$$\langle JxB\rangle_x = f_{JxB}\langle J_y\rangle\langle B\rangle$$

and Lorentz power

$$\langle J.E\rangle_x = f_{J.E}\langle J_y\rangle\langle E_y\rangle$$

where f_{JxB} and $f_{J.E}$ are electrical form factors.

By some substitutions and manipulations, the simplified, analytical model which consists of a hyperbolic set of three coupled, first-order, nonlinear partial differential equations is obtained

$$\frac{\partial}{\partial t}(\rho A) + \frac{\partial}{\partial x}(\rho UA) = 0 \quad , \tag{4}$$

$$\frac{\partial}{\partial t}(\rho UA) + \frac{\partial}{\partial x}(\rho U^2A) = -A\left(\frac{\partial p}{\partial x} - f_{JxB}\langle J_y\rangle\langle B\rangle\right) \quad , \tag{5}$$

$$\frac{\partial}{\partial t}[\rho(\varepsilon+U^2)A] + \frac{\partial}{\partial x}(\rho Uh_oA) = f_{J.E}\langle J_y\rangle\langle E_y\rangle A + q_wP \quad . \tag{6}$$

The three dependent variables selected are the mass density ρ, the axial flow velocity U and the temperature T. The MHD model in matrix form is

$$
\begin{bmatrix} 1 & 0 & 0 \\ U & \rho & 0 \\ (c_p-R)T+U^2 & 2U\rho & (c_p-R)\rho \end{bmatrix}
\begin{bmatrix} \rho_t \\ U_t \\ T_t \end{bmatrix} +
$$

$$
\begin{bmatrix} U & \rho & 0 \\ U^2+RT & 2U\rho & R\rho \\ c_pUT+U^3/2 & c_p\rho T+3U^2\rho/2 & c_p\rho U \end{bmatrix}
\begin{bmatrix} \rho_x \\ U_x \\ T_x \end{bmatrix} =
$$

$$
\begin{bmatrix} -\frac{\rho U}{A}\frac{\partial A}{\partial x} \\ -\frac{\rho U^2}{A}\frac{\partial A}{\partial x} + f_{JxB}\langle J_y\rangle\langle B\rangle \\ -\left(\frac{c_p\rho UT}{A} + \frac{\rho U^3}{2A}\right)\frac{\partial A}{\partial x} + f_{J.E}\langle J_y\rangle\langle E_y\rangle + \frac{q_wP}{A} \end{bmatrix} . \tag{7}
$$

which can be written in local balance equation form

$$
\underline{C}(\underline{Q})\underline{Q}_t + \underline{D}(\underline{Q})\underline{Q}_x = \underline{d}(\underline{Q}) \quad , \tag{8}
$$

where $\underline{Q}_t$ and $\underline{Q}_x$ are the time derivative and the spatial derivative vectors of the dependent variable vector, $\underline{Q}$. The vector of dependent variables is

$$
\underline{Q} = \begin{bmatrix} \rho(x,t) \\ U(x,t) \\ T(x,t) \end{bmatrix}
$$

and the MHD specific terms appear in $\underline{d}$, the vector of production/absorption terms.

In general, equation (8) is a nonlinear, nonhomogeneous, coupled hyperbolic system of partial differential equations, e.g., the equations describing one-dimensional compressible flow. Premultiplication by $\underline{C}^{-1}$ simplifies equation (8) to

$$\underline{Q}_t + \underline{A}\underline{Q}_x = \underline{f} \tag{9}$$

where $\underline{A} = \underline{C}^{-1}\underline{D}$ and $\underline{f} = \underline{C}^{-1}\underline{d}$.

2. Conventional Application of Numerical Method of Lines

The Numerical Method of Lines is a discretization technique for solving partial differential equations. The Numerical Method of Lines can be applied to equation (9) by using finite-difference replacements for the spatial derivatives. Thus the partial differential equations are converted to a set of coupled ordinary differential equations in time derivatives only.

The Method of Lines comprises the spatial derivative algorithms and the numerical integrators for integration of ordinary differential equations. The Method of lines has been applied successfully to partial differential equations for both stiff systems and nonstiff systems. see Johnson and Hindmarsh [3] for a stiff system application.

The MHD model is a nonstiff system. The spatial derivatives are replaced by the finite difference subroutines, DSS002 for a three-point centered difference formula, DSS012 for a two-point upwind difference formula and DSS018 for a four-point biased upwind difference formula, see Dissinger, Schiesser and Johnson [4]. All the temporal integrations are performed by a suitably powerful ODE system solver - LSODE [5].

For the first one meter of the MHD channel , the conventional application of the Numerical Method of Lines to 11 fixed, discrete points equally spaced along the channel, produces a set of 33 coupled, temporal, nonlinear, first-order, initial value, ordinary differential equations.

The numerical results from the application of the Method of Lines with upwind (DSS012) and biased upwind (DSS018) approximations exhibit unstable solutions during the time 0. to 0.002 seconds .

For the three-point centered finite difference formula replacement used, the solution is numerically stable, but severely distorted. Table 1. presents the eleven-point solutions for conservation of mass, linear momentum and total energy equations at time = 0.002 sec. and at time = 0.01 sec., when using a centered finite-difference formula to replace the spatial derivatives. The solution shows severe ripple at time = 0.01 sec.

These solutions may be compared with the solutions from the method of Pseudocharacteristics, see Table 2. At time = 0.002 sec., the solution is close to the solution of the Pseudocharacteristic method, but the longer the simulation runs, the more distorted the solution obtained by the conventional application of the Method of Lines becomes.

The difficulty of applying the Method of Lines to the MHD model is mainly that discontinuities can propagate in both downstream and upstream directions. In general, hyperbolic problems can be successfully solved by the Method of Lines with upwind or biased finite difference formulas to replace the spatial derivatives. But the spatial derivatives replacements used must be biased in the directions of propagation.

	Density kg/m^3	Velocity m/s	Temperature °K
Time=0.002 sec.			
x=0.0m	.57139	782.73	2697.3
x=0.1m	.59637	740.40	2711.0
x=0.2m	.57440	771.57	2703.9
x=0.3m	.57535	766.34	2706.8
x=0.4m	.56794	774.12	2706.1
x=0.5m	.56280	777.91	2706.8
x=0.6m	.55708	782.42	2707.3
x=0.7m	.55148	786.66	2707.7
x=0.8m	.54600	790.79	2707.4
x=0.9m	.54041	794.73	2707.4
x=1.0m	.53472	798.49	2708.0
NST=48	NFE=79	NEJ=0	STEP SIZE= 2.863E-5
Time=0.01 sec.			
x=0.0m	.57139	782.73	2697.3
x=0.1m	.66898	603.00	2747.3
x=0.2m	.56259	789.18	2698.6
x=0.3m	.64157	639.82	2740.3
x=0.4m	.55101	798.31	2699.1
x=0.5m	.60956	684.07	2731.1
x=0.6m	.53646	812.41	2697.9
x=0.7m	.57068	740.37	2718.6
x=0.8m	.51374	838.55	2693.4
x=0.9m	.51925	819.89	2699.7
x=1.0m	.48193	882.97	2684.0
NST=209,	NFE=347,	NEJ=0	STEP SIZE= 9.564E-5

Table 1. The 11-Point Solutions from the Conventional Numerical Method of Lines

3. The Background of Numerical Methods of Charactericteristics

Hyperbolic equations have distinct real eigenvalues which represent the directions of propagation. For the solution of problems in which eigenvalues of both signs exist, misaligned biasing will induce instability. As a result of this directional nature of hyperbolic equations, the numerical methods of Characteristics for decoupling sets of one-dimensional hyperbolic partial differential equations have been developed.

Methods may be either of two kinds. One employs differencing along the characteristic curves, the other employs differencing on a fixed grid. The former includes the method of differences along a curvilinear net , see Courant, Isaacson and Rees [6], and the method of wave tracing, see Hancox and Banerjee [7]. The latter includes the method of differences on a rectangular net by Courant et al,[6], and the characteristic finite-difference (CFD) procedure of Hancox and Mcdonald [8].

In the method of differences along a curvilinear net, a set of first-order hyperbolic partial differential equations is discretized into

$$\sum_{i=1}^{n} M^{ij}(Q^i_t + \lambda^j Q^i_x) = L^i , \quad j=1, \ldots, n \tag{10}$$

where

$$\lambda^j = \frac{dx}{dt} \tag{11}$$

are the j^{th} characteristic directions.

For each equation of (10), the variables Q^i are differentiated in the characteristic direction λ^j, that is

$$\frac{dQ}{dt} = Q_t^i + \lambda^j Q_x^i \tag{12}$$

and by substitution of (12) into (10),

$$\sum_{i=1}^{n} M^{ij} \frac{dQ^i}{dt} = L^i \quad . \tag{13}$$

The derivatives in equation (10) are directly replaced along the characteristic directions by first-order finite differences.

The wave tracing method has been applied to the hyperbolic partial differential equations in the form of equation (9).The method involves transforming equation (9) along the characteristic directions that are the eigenvectors of matrix $\underline{A}$. The two sets of ordinary differential equations are defined by

the characteristic equations

$$\underline{\frac{dx}{dt}} = \underline{\lambda} \tag{14}$$

and the compatibility equations which result from the transfomation of equation (9)

$$\underline{\frac{MdQ}{dt}} = \underline{L} \tag{15}$$

where $\underline{M}$ and $\underline{L}$ are the coefficient vectors.

The characteristic equations and the compatibility equations along those characteristics are solved recursively based on a first-order finite difference approximation.

The basis of the methods of differencing along the characteristic directions is that the solution is defined by initial and boundary conditions, and two sets of ordinary differential equations, the characteristic equations and the compatibility equations, such as equations (11) and (13), in methods of differencing along a curvilinear net, and equations (14) and (15) in the method of wave tracing.

The wave tracing method has been applied to the one-dimensional flow-boiling problem, see Hancox and McDonald [8].

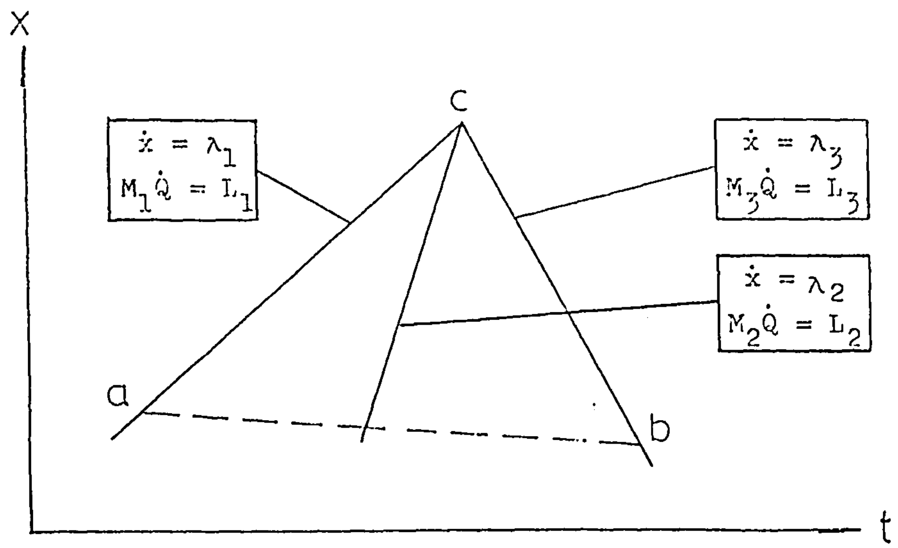

Figure 2. Wave Tracing Algorithm to Advance Solution along the Characteristics

As shown in Figure 2, six of the required ten equations can be obtained from first-order finite difference approxmations to the characteristic and compatibility equations, and between points a and b there are four equations obtained from linear interpolations along the adjacent characteristics λ_2. Therefore the solution involves linear interpolation and iterative solution of a total of ten algebraic equations. At a discontinuous phase transition, twenty nonlinear algebraic equations have to be matched by iteration. However, the wave tracing method allows discontinuities to propagate without diffusion and the numerical solutions obtained can approximate exact solutions closely. But the method is complicated to program, expensive to execute and difficult to apply to any except the simplest geometries. See Hancox and Banerjee [7] for a third-order application and Ferch [9] for a similar fifth-order application.

In the methods of characteristics on a fixed grid, i.e., the method on the rectangular net and the characteristic finite-difference procedure, the basis is the transformation of the original set of equations (9) into the following a set of canonical equations of form (16) with separated and known propagation directions which permit appropriate biasing, that is,

$$\underline{BQ}_t + \underline{\Lambda BQ}_x = \underline{B}\ \underline{f} \qquad (16)$$

where $\underline{\Lambda}$ is the diagonal matrix of eigenvalues of $\underline{A}$ and $\underline{B}$ is the transformation matrix obtained from :

$$\underline{B}\ \underline{A}\ \underline{B}^{-1} = \underline{\Lambda} \quad . \tag{17}$$

The methods are based on replacing derivatives by first-order finite-differences in time and space. The following finite difference algorithm may be written at point k:

if $_i$ is positive

$$B_{ik}\frac{dQ_k}{dt} + \lambda_i\ B_{ik}\frac{Q_k-Q_{k-1}}{x_k-x_{k-1}} = B_{ik}f_k \quad , \tag{18}$$

and if $_i$ is negative

$$B_{ik}\frac{dQ_k}{dt} + \lambda_i\ B_{ik}\frac{Q_{k+1}-Q_k}{x_{k+1}-x_k} = B_{ik}f_k \quad . \tag{19}$$

The characteristic finite difference procedure has been applied to a one dimensional flow-boiling problem, see Hancox and Banerjee [6]. The method produces stable solutions and low cost computation, but introduces numerical diffusion.

The reason diffusion is introduced is that the finite difference algorithm using a fixed rectangular grid of points violates the domain of dependence requirements. The domain of dependence is the region bounded by λ_1 and λ_3 characteristic curves, see Figure 2. In the wave tracing method, solution point c is at the intersection of the characteristic curves $dx/dt= \lambda_i$ (i=1,2,3) that originate from previously determined solution points a and b. It is affected only by information contained within the domain of dependence, while, in the finite difference on a fixed grid method, the values of the dependent variables at grid points outside the domain of dependence will inevitably enter the difference equations, then accurate finite difference approximation solutions only could be produced in the limit as time and space discretizations approach zero.

4. The Pseudocharacteristic Numerical Method of Lines

The method of Pseudocharacteristics with discretization by the Method of Lines extends the characteristic finite difference concept to a canonical form, which combines accomodation of the directional properties of the hyperbolic equations with higher-order discretization approximations in time and space. The propagation directions are separated and directional biasing can be applied appropriately.

The Pseudocharacteristic equations for the temporal ordinary differential equations can be obtained either by solving the linear system, see Carver [1], or by matrix transformation.

(1) Obtain the ordinary differential equations by solving the linear system.

The scalar equation in (12) can be written as

$$B_{i1}Q_{t1}+B_{i2}Q_{t2}+B_{i3}Q_{t3} = -\lambda_i(B_{i1}Q_{x1}+B_{i2}Q_{x2}+B_{i3}Q_{x3}) + (B_{i1}f_1+B_{i2}f_2+B_{i3}f_3) \qquad (20)$$

$i = 1, 2, 3.$

The spatial derivatives Q_{x1}, Q_{x2} and Q_{x3} can be replaced by higher-order biased approximations according to the sign of the eigenvalues λ_i. The Pseudocharacteristic equations may be obtained by solving the i^{th} linear system equations (19) for the time derivatives Q_{t1}, Q_{t2} and Q_{t3} in explicit form without matrix inversion. The method has been applied to several sets of first-order hyperbolic equations.

Kolev and Katkovsky [11], obtained comparable performance from the method of characteristics on a fixed grid using a two-step Lax-Wendroff technique and the method of Pseudocharacteristics using the GEAR software package for temporal integration and a four-point upwind biased finite difference approximation for the spatial derivatives. The results from the method of Pseudocharacteristics exhibited good accuracy, less numerical diffusion and less computer time for execution.

(2) Obtain the ordinary differential equations by matrix transformation.

The Pseudocharacteristic equation form is based on the transformation of equation (16) to a canonical form which is

$$\underline{W}_t + \underline{W}_x = \underline{g} \quad . \tag{21}$$

where $\underline{W} = \underline{B}\ \underline{Q}$

The scalar equation in (21) can be written as

$$W_{ti} + \lambda_i W^i_{xi} = g_i \ , \quad i = 1,\ 2,\ 3. \tag{22}$$

where the superscript indicates which eigenvalue is used to establish the direction of biasing.

In terms of original state variables

$$W^i_{xi} = B_{i1}Q^i_{x1} + B_{i2}Q^i_{x2} + B_{i3}Q^i_{x3} \ , \quad i = 1,2,3 \quad . \tag{23}$$

Therefore equation (16) transforms into the decoupled form

$$\underline{BQ}_t + \underline{Q}^*_x = \underline{g} \tag{24}$$

which $\underline{Q}_x^*$ can be repreasented in vector form

$$\underline{Q}_x^* = \begin{bmatrix} B_{11}\left(\frac{\partial Q_1}{\partial x}\right)_{\lambda_1} + B_{12}\left(\frac{\partial Q_2}{\partial x}\right)_{\lambda_1} + B_{13}\left(\frac{\partial Q_3}{\partial x}\right)_{\lambda_1} \\ B_{21}\left(\frac{\partial Q_1}{\partial x}\right)_{\lambda_2} + B_{22}\left(\frac{\partial Q_2}{\partial x}\right)_{\lambda_2} + B_{23}\left(\frac{\partial Q_3}{\partial x}\right)_{\lambda_2} \\ B_{31}\left(\frac{\partial Q_1}{\partial x}\right)_{\lambda_3} + B_{32}\left(\frac{\partial Q_2}{\partial x}\right)_{\lambda_3} + B_{33}\left(\frac{\partial Q_3}{\partial x}\right)_{\lambda_3} \end{bmatrix} .$$

Define $\underline{A}^* = \underline{B}^{-1}\underline{\Lambda} = \underline{AB}^{-1}$, then

$$\underline{Q}_t + \underline{A}^*\underline{Q}_x^* = \underline{f} \quad . \tag{25}$$

Equation (25) is the set of ordinary differential equations in matrix form obtained by inverting transformation matrix $\underline{B}$ without solving the linear system of equations. The Method of Lines is used to discretize this set of partial differential equations with the stipulation that each spatial derivative must be biased according to the sign of the associated eigenvalue and weighted by the elements of the transformation matrix. This is a basic difference from equation (9) obtained by the conventional application of the Method of Lines.

To apply the Pseudocharacteristic method to the MHD model of the channel section, the transformation matrix $\underline{B}$ can be any nontrivial solution of equation (17). We define the transformation matrix as

$$\underline{B} = \begin{bmatrix} B_{11} & B_{12} & 1 \\ B_{21} & B_{22} & 1 \\ B_{31} & B_{32} & 1 \end{bmatrix} .$$

the Pseudocharacteristic form of equation (16) is

$$\begin{bmatrix} B_{11} & B_{12} & 1 \\ B_{21} & B_{22} & 1 \\ B_{31} & B_{32} & 1 \end{bmatrix} \begin{bmatrix} \rho_t \\ U_t \\ T_t \end{bmatrix} = - \begin{bmatrix} \lambda_1 & 0 & 0 \\ 0 & \lambda_2 & 0 \\ 0 & 0 & \lambda_3 \end{bmatrix} \begin{bmatrix} B_{11} & B_{12} & 1 \\ B_{21} & B_{22} & 1 \\ B_{31} & B_{32} & 1 \end{bmatrix} \begin{bmatrix} \rho_x \\ U_x \\ T_x \end{bmatrix}$$

$$+ \begin{bmatrix} B_{11} & B_{12} & 1 \\ B_{21} & B_{22} & 1 \\ B_{31} & B_{32} & 1 \end{bmatrix} \begin{bmatrix} f_1 \\ f_2 \\ f_3 \end{bmatrix} . \qquad (26)$$

To obtain the ordinary differential equations by solving the linear system, equation (26) can be written in expanded form with spatial derivatives biased according to the sign of eigenvalues, which is

$$B_{11}\rho_t+B_{12}U_t+T_t = - \lambda_1(B_{11}\rho_{x+}+B_{12}U_{x+}+T_{x+}) + B_{11}f_1+B_{12}f_2+f_3 \qquad (27)$$

$$B_{21}\rho_t+B_{22}U_t+T_t = - \lambda_2(B_{21}\rho_{x0}+B_{22}U_{x0}+T_{x0}) + B_{21}f_1+B_{22}f_2+f_3 \qquad (28)$$

$$B_{31}\rho_t+B_{32}U_t+T_t = - \lambda_3(B_{31}\rho_{x-}+B_{22}U_{x-}+T_{x-}) + B_{31}f_1+B_{32}f_2+f_3 \quad . \qquad (29)$$

The subscripts "+", "-" and "0" indicate the signs of eigenvalues. The replacement of spatial derivatives with the signs "0" and "+" is governed by the positive eigenvalue and "-" by the negative eigenvalue. In case the eigenvalue is equal to zero, the spatial derivative is replaced by the centered finite difference formula.

Thus the ordinary differential equations in terms of $_t$, U_t and T_t are obtained by solving linear system equations (27), (28) and (29) simultaneously. This requires more manipulations than the matrix transformation procedure.

The following is a portion of the computer program for solving the linear system:

```
  FIND THE ELEMENTS OF B

 B12=(A(1,2)*A(3,1)+A(3,2)*(EGVAL1-A(1,1)))/
+    ((EGVAL1-A(1,1)*(EGVAL1-A(2,2))
+    -A(1,2)*A(2,1))
 B22=(A(1,2)*A(3,1)+A(3,2)*(EGVAL2-A(1,1)))/
+    ((EGVAL2-A(1,1))*(EGVAL2-A(2,2))
+    -A(1,2)*A(2,1))
 B32=(A(1,2)*A(3,1)+A(3,2)*(EGVAL3-A(1,1)))/
+    ((EGVAL3-A(1,1))*(EGVAL3-A(2,2))
+    -A(1,2)*A(2,1))
 B11=(A(3,1)+B12*A(2,1))/(EGVAL1-A(1,1))
 B21=(A(3,1)+B22*A(2,1))/(EGVAL2-A(1,1))
 B31=(A(3,1)+B32*A(2,1))/(EGVAL3-A(1,1))

 DENOM=B11*B22+B12*B31+B21*B32-B12*B21-B11*B32-B22*B31

  CALCULATE RIGHTHAND SIDES OF EQUATIONS 27-29

 REQ27=-EGVAL1*(B11*RHOX1+B12*UX1+TX1)
+       +B11*F1+B12*F2+F3
 REQ28=-EGVAL2*(B21*RHOX2+B22*UX2+TX2)
+       +B21*F1+B22*F2+F3
 REQ29=-EGVAL3*(B31*RHOX3+B32*UX3+TX3)
+       +B31*F1+B32*F2+F3

  OBTAIN A SET OF TEMPORAL ODES BY
  SOLVING EQUATIONS 27-29

 RHOT(I)=((B22-B32)*REQ27+(B21-B22)*REQ29
+         +(B32-B12)*REQ28)/DENOM
 TT(I)=((B22*B31-B21*B32)*REQ27+(B12*B21-B22*B11)
+       *REQ29 +(B11*B32-B12*B31)*REQ28)/DENOM
 UT(I)=(B21*RHOT(I)-TT(I)+REQ28)/B22
```

To obtain the ordinary differential equations by matrix transformation without solving the linear system equations, equation (25) can written as

$$\underline{Q}_t = - \underline{B}^{-1}\underline{\Lambda B Q}_x + \underline{f} \quad , \tag{30}$$

or in explicit form

$$\begin{bmatrix} \rho_t \\ U_t \\ T_t \end{bmatrix} = - \begin{bmatrix} B_{11} & B_{12} & 1 \\ B_{21} & B_{22} & 1 \\ B_{31} & B_{32} & 1 \end{bmatrix}^{-1} \begin{bmatrix} \lambda_1(B_{11}\rho_{x+} + B_{12}U_{x+} + T_{x+}) \\ \lambda_2(B_{21}\rho_{x0} + B_{22}U_{x0} + T_{x0}) \\ \lambda_3(B_{31}\rho_{x-} + B_{32}U_{x-} + T_{x-}) \end{bmatrix} + \begin{bmatrix} f_1 \\ f_2 \\ f_3 \end{bmatrix} \tag{31}$$

See the details of the MHD model computer program coding below. The program provides a way, in general, to solve a set of first-order, nonlinear partial differential equations in time and space by the method of Pseudocharacteristics.

FIND THE ELEMENTS OF B

```
 B12=(A(1,2)*EGVAL1-A(1,2)*A(3,3)+A(1,3)*A(3,2))/
+     (A(1,3)*EGVAL1+A(1,2)*A(2,3)-A(2,2)*A(1,3))
 B22=(A(1,2)*EGVAL2-A(1,2)*A(3,3)+A(1,3)*A(3,2))/
+     (A(1,3)*EGVAL2+A(1,2)*A(2,3)-A(2,2)*A(1,3))
 B32=(A(1,2)*EGVAL3-A(1,2)*A(3,3)+A(1,3)*A(3,2))/
      (A(1,3)*EGVAL3+A(1,2)*A(2,3)-A(2,2)*A(1,3))
 B11=(A(2,1)*EGVAL1-A(2,1)*A(3,3)+A(2,3)*A(3,1))/
+     (A(2,3)*EGVAL1-A(1,1)*A(2,3)+A(2,1)*A(1,3))
 B21=(A(2,1)*EGVAL2-A(2,1)*A(3,3)+A(2,3)*A(3,1))/
+     (A(2,3)*EGVAL2-A(1,1)*A(2,3)+A(2,1)*A(1,3))
 B31=(A(2,1)*EGVAL3-A(2,1)*A(3,3)+A(2,3)*A(3,1))/
+     (A(2,3)*EGVAL3-A(1,1)*A(2,3)+A(2,1)*A(1,3))
```

FIND THE INVERSE OF B

```
 DENOM=B11*B22*B33-B21*B32*B13+B12*B23*B31
+      -B13*B22*B31-B12*B21*B33-B23*B32*B11

 BI11=EGVAL1*(B22*B33-B23*B32)/DENOM
```

```
BI12=EGVAL2*(B13*B32-B12*B33)/DENOM
BI13=EGVAL3*(B12*B23-B13*B22)/DENOM
BI21=EGVAL1*(B23*B31-B21*B33)/DENOM
BI22=EGVAL2*(B11*B33-B13*B31)/DENOM
BI23=EGVAL3*(B13*B21-B11*B23)/DENOM
BI31=EGVAL1*(B21*B32-B22*B31)/DENOM
BI32=EGVAL2*(B12*B31-B11*B32)/DENOM
BI33=EGVAL3*(B11*B22-B12*B21)/DENOM

  A SET OF TEMPORAL ODES

RHOT(I)=-B11*(B11*RHOX1+B12*UX1+B13*TX1)
        -B12*(B21*RHOX2+B22*UX2+B23*TX2)
        -B13*(B31*RHOX3+B32*UX3+B33*TX3)
UT(I)  =-B21*(B11*RHOX1+B12*UX1+B13*TX1)
+       -B22*(B21*RHOX2+B22*UX2+B23*TX2)
+       -B23*(B31*RHOX3+B32*UX3+B33*TX3)
T(I)   =-B31*(B11*RHOX1+B12*UX1+B13*TX1)
+       -B32*(B21*RHOX2+B22*UX2+B23*TX2)
+       -B33*(B31*RHOX3+B32*UX3+B33*TX3)
```

The numerical results from the two ways (1) and (2) are identical.

If equation (9) is solved by the Method of Lines and equation (25) is solved by the method of Pseudocharacteristics with the same finite difference replacement for spatial derivatives, e.g., by a centered finite-difference formula, the numerical solutions are identical, that means equation (25) reverts to equation (9). This is a distinction of the Pseudocharacteristic method, that more accurate, stable solutions of hyperbolic partial differential equations can be obtained by the Pseudocharacteristic method without any additional impact on the solutions..

	Density kg/m^3	Velocity m/s	Temperature °K
Time=0.002 sec.			
x=0.0m	.57139	782.73	2697.3
x=0.1m	.58955	750.96	2708.0
x=0.2m	.57798	765.61	2705.5
x=0.3m	.57386	768.31	2706.3
x=0.4m	.56813	773.38	2706.5
x=0.5m	.56263	777.87	2706.8
x=0.6m	.55706	782.29	2707.1
x=0.7m	.55144	786.53	2707.4
x=0.8m	.54581	790.61	2707.8
x=0.9m	.54018	794.57	2708.1
x=1.0m	.53456	798.40	2708.5
NST=60	NFE=105	NJE=0	STEP SIZE= 2.65E-5
Time=0.01 sec.			
x=0.0m	.57139	782.73	2697.3
x=0.1m	.63294	685.62	2727.1
x=0.2m	.60089	730.55	2715.5
x=0.3m	.60200	725.08	2718.7
x=0.4m	.59148	737.25	2716.7
x=0.5m	.58491	743.15	2716.5
x=0.6m	.57684	751.29	2715.6
x=0.7m	.56903	758.86	2714.8
x=0.8m	.56070	767.04	2713.9
x=0.9m	.55194	775.83	2712.8
x=1.0m	.54274	785.90	2711.4
NST=233	NFE=431	NJE=0	STEP SIZE= 6.45E-5

Table 2. The 11-Points Solutions of the Pseudo-characteristic Method.

5. Computer Program for MHD Model

The application of the method of Pseudocharacteristics with the Method of Lines to n fixed, discrete points, uniformly distributed along the channel, with the spatial derivatives replaced by fourth-order biased finite difference formulas produces a set of 3n coupled nonlinear, first-order ordinary differential equations which can be solved by the numerical integrator LSODE [5]. LSODE is a convenient, flexible and portable integrator which has many options and capabilities.

The program for the MHD model which calls LSODE is written as the follows:

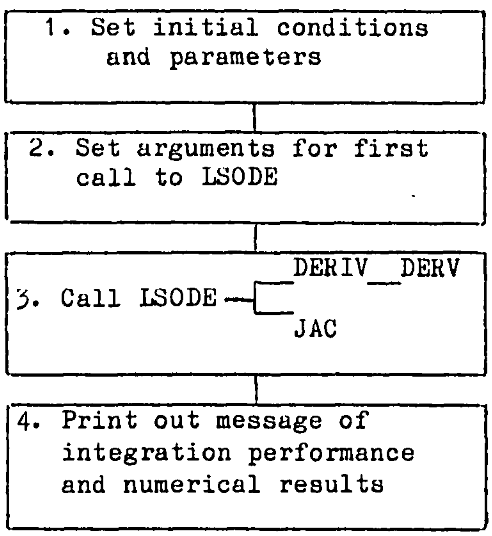

Block 1 is executed by a subroutine INITAL that supplies the initial conditions and sets system parameters. The property data for the MHD channel section are approximated by polynomial functions which are obtained from curve regression and the errors are less than 10%.

Block 2 supplies the following input arguments on the first call to LSODE.

NEQ = Number of first-order ordinary differential equations.

Y = The vector of dependent variables.

TOUT = First point where output is desired.

ITOL = An indicator for the type of error control.

RTOL = Relative tolerance parameter.

ATOL = Absolute tolerance parameter.

RWORK= Real work array of length (=20+16*NEQ).

IWORK= Integer work array.

LIW = Declared length of IWORK.

LRW = Declared length of RWORK.

ISTATE=An index used for input and output to specify the state of calculation.

ITASK= An index specifying the task to be performed.

IOPT = An integer flag.

MF = The method flag.

Block 3 is ready to call LSODE:

```
CALL LSODE (DIRVE,NEQ,Y,TIME,TOUT,ITOL,RTOL,ATOL,
ITASK,ISTATE,IOPT,RWORK,LRW,IWORK,LIW,JAC,MF)
```

Block 4 will print out the numerical result and the messages from integrator LSODE. Some of the messages are:

NST = The number of steps taken
for the problem so far.

NFE = The number of dQ/dt evaluations
for the problem so far.

NEJ = The number of Jacobian evaluations
for the problem so far.

The integrator performance can be diagnosed from these messages.

LSODE requires two external subroutines, DERIV and JAC. Subroutine JAC computes the Jacobian matrix for stiff systems. The MHD model system is not stiff, therefore JAC is not used and the program passes a dummy name. Subroutine DERIV followed by subroutine DERV define the ordinary differential equation system, i.e., $d\underline{Q}/dt$. Subroutine DERV is the most important part of the application of the method of Pseudocharacteristics. Subroutine DERV is formulated as follows:

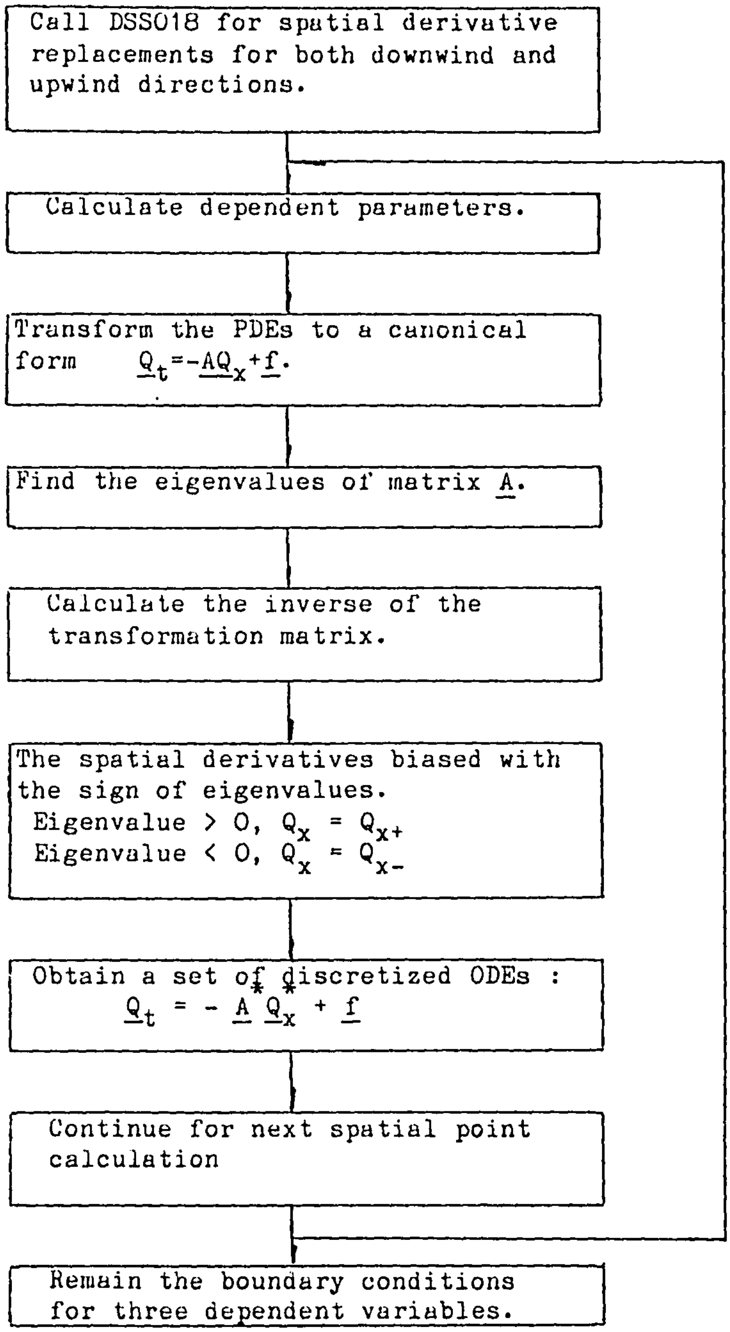
Call DSS018 for spatial derivative replacements for both downwind and upwind directions.
Calculate dependent parameters.
Transform the PDEs to a canonical form $\underline{Q}_t = -\underline{A}\underline{Q}_x + \underline{f}$.
Find the eigenvalues of matrix $\underline{A}$.
Calculate the inverse of the transformation matrix.
The spatial derivatives biased with the sign of eigenvalues.
Eigenvalue > 0, $Q_x = Q_{x+}$
Eigenvalue < 0, $Q_x = Q_{x-}$
Obtain a set of discretized ODEs :
$\underline{Q}_t = - \underline{A}^* \underline{Q}_x^* + \underline{f}$
Continue for next spatial point calculation
Remain the boundary conditions for three dependent variables.

Computer execution is efficient for the method of Pseudocharacteristics. The time to run for the Method of Lines with a three-point centered finite difference formula is 13.1 seconds and the time to run for the method of Psedocharacteristics with the four-point biased formula is 13.6 seconds.

The advantages of the method of Pseudocharacteristics are the ease of formulation, flexibility of selection of spatial derivative replacements and compatibility with general-purpose software like LSODE, which is a reliable, high-order, error controlled, integration package.

6. System Jacobian Maps and Eigenvalues

There are some comparisons that can be made between the conventional Method of Lines and the method of Pseudocharacteristics using Jacobian maps and the eigenvalues of the Jacobian matrices for the discretized ordinary differential equation systems.

If the Method of Lines is used to discretize the simplified MHD model in the form of equation (9) and centered, three-point finite difference approximations are used to replace the spatial derivatives, a set of initial-value ODEs result suitable for integration by LSODE. If eleven solution points are distributed uniformly along the first one meter of the channel and the integration is run long enough for the solution to approach steady state, the Jacobian map of the ODE system will be as shown in Figure 3. If the MHD model is analytically converted to the form of equation (25), and a four-point upwind biased finite difference approximation used in the discretization, the steady state Jacobian map is as shown in Figure 4.

In Figure 3 and Figure 4, Rows 1 through 11 represent the discretized density equations, Rows 12 through 22 represent the discretized velocity equations and Rows 23 through 33 represent the discretized temperature equations. The entries in the Jacobian map (m_{ij}) indicate the magnitudes of the nonzero elements in the Jacobian (J_{ij}) according to $|J_{ij}| \sim$ 10**(m_{ij}-5). See Dissinger, Schiesser and Johnson [4].

The upper right block of nonzero elements in Figure 4 is not present in Figure 3, and the block bandwidths in Figure 4 are bigger than in Figure 3. In general, transformation to the Pseudocharacteristic form decreases the number of empty blocks with the sequential equation Jacobian map, and increases the block bandwidths. The bandwidth is increased by the likelihood of both a left-biased finite difference algorithm plus a right-biased finite difference algorithm, since $\underline{Q}_x^*$ in equation (25) contains both. The number of diagonals within the banded blocks is determined by the spatial derivative replacements used and the magnitudes are determined by the original problem. The production/absorption terms affect the main diagonals of the blocks only.

The ordinary differential equations can be reordered to reduce the Jacobian bandwidth. Figure 5 shows a reordered Jacobian map for the discretized standard form, i.e., equation (9) of the MHD model. Figure 6 is the reordered Jacobian map for the discretized Pseudocharacteristic form, i.e., equation (25) of the MHD model. Figure 6 shows a Jacobian map similar to Figure 5, but with a slightly greater bandwidth.

Table (3a) is the list of eigenvalues of the Jacobian of discretized equation (9). Table (3b) is the list of eigenvalues of the Jacobian of discretized equation (25) at steady state.

The stiffness ratio is calculated by dividing the largest real part of an eigenvalue by the smallest real part of an eigenvalue, see Dissinger, Schiesser and Johnson [4], which is expressed as:

$$\text{Stiffness Ratio} = \frac{|\max(\mathrm{Re})|}{|\min(\mathrm{Re})|}$$

The stiffness ratio for the ordinary differential equations resulting from the standard Method of Lines discretization with centered algorithm used to approximate the spatial derivatives is 65. The stiffness ratio for the ordinary differential equations resulting from the method of Pseudocharacteristics with fourth-order biased upwind algorithm is 101. Therefore, in this case, the method of Pseudocharacteristics increases the stiffness.

```
              11111111112222222222333
     123456789012345678901234567890123
 1   
 2    68         35
 3    878        545
 4     868        535
 5      878        545
 6       868        535
 7        878        545
 8         878        535
 9          878        545
10           878        545
11           899        555
12   
13    99         68         68
14    999        878        868
15     999        868        868
16      999        878        868
17       999        868        868
18        999        878        878
19         999        878        868
20          999        878        878
21           999        878        868
22           999        899        888
23   
24    99         57         58
25    999        767        868
26     989        767        868
27      999        767        868
28       979        666        868
29        999        777        868
30         999        767        868
31          999        777        868
32           999        767        868
33           999        788        899
```

Figure 3. Jacobian Map of Discretized Equation (9) for an 11-point Grid by Method of Lines

```
              111111111122222222223333
     123456789012345678901234567890123
 1
 2   8888       5555
 3   88887      45553      34443
 4    88887      45553      34443
 5     88887      45553      34443
 6      88887      45553      34443
 7       88887      45553      34443
 8        88887      45553      33433
 9         88887      45553      33433
10          8888       4555
11          8999       5565
12
13   9999       8888       7887
14   99999      88887      78886
15    99999      88887      78886
16     99999      88887      78886
17      99999      88887      78886
18       99999      88887      78886
19        99999      88887      78886
20         99999      88887      78886
21          9999       8888       7887
22          9999       8999       7888
23
24   9999       6676       8888
25   99999      67776      88886
26    99999      67776      88886
27     99999      67766      88886
28      99999      67766      88886
29       99999      67766      88886
30        99999      67766      88886
31         99999      67766      88886
32          9999       6777       8888
33          9999       7788       8999
```

Figure 4. Jacobian Map of Discretized Equation (25) for an 11-point Grid by Pseudocharacteristics

```
                1111111111222222222233333
       123456789012345678901234567890123
  1
  2
  3
  4       63 85
  5       966988
  6       955978
  7       85 74 85
  8       988976988
  9       978966978
 10          85 63 85
 11          988966988
 12          978866978
 13             85 74 85
 14             988976988
 15             978966978
 16                85 63 85
 17                988966988
 18                968766968
 19                   85 74 85
 20                   988977988
 21                   978976978
 22                      85 73 85
 23                      988976988
 24                      978966978
 25                         85 74 85
 26                         988977988
 27                         978976978
 28                            85 74 85
 29                            988976988
 30                            978966978
 31                            85 95 95
 32                            988998998
 33                            978989989
```

Figure 5. Jacobian Map of Discretized Equation (9) Interleaved

```
             111111111122222222223333
    123456789012345678901234567890123
 1
 2
 3
 4  85 85 85 85
 5  987988988987
 6  968968978968
 7  843854854854733
 8  987988988988976
 9  968978978978966
10     843854854854733
11     987988988988976
12     968978978978966
13        843854854854733
14        987988988988976
15        968978978968966
16           843854854854733
17           987988988988976
18           968978978968966
19              843854854854733
20              987988988988976
21              968978978968965
22                 843853854853733
23                 987988988988976
24                 968978978968966
25                    843853854853733
26                    987988988988976
27                    968978978968966
28                       84 85 85 85
29                       987988988987
30                       968978978978
31                       85 95 96 95
32                       987998998998
33                       978979989989
```

Figure 6. Jacobian Map of Discretized Equation (25) Interleaved

-548+j14830
-548-j14830
-1297+j12640
-1297-j12640
-10310
-2343+j9392
-2343-j9392
-363+j7301
-363-j7301
-681+j6209
-681-j6209
-3147+j5323
-3147-j5323
-1200+j4690
-1200-j4690
-4062+j995
-4062-j995
-1464+j2726
-1464-j2726
-159+j1529
-159-j1529
-1342
-202+j1109
-202-j1109
-253+j717
-253-j717
-315+j174
-315-j174
-433+j376
-433-j376

(a) Eigenvalues for Equation 9

$$\text{Stiffness ratio} = \frac{10310}{158.6} = 65$$

-6013+j16700
-6013-j16700
-7197+j16160
-7197-j16160
-8874+j11960
-8874-j11960
-10270+j6965
-10270-j6965
-10410+j1909
-10410-j19090
-3617+j8100
-3617-j8100
-2930+j7853
-2930-j7853
-4372+j5902
-4372-j5902
-5069+j3450
-5069-j3450
-5196+j988
-5196-j988
-917+j1859
-917-j1859
-805+j1414
-805-j1414
-566+j852
-566-j852
-103+j493
-103-j493
-184+j247
-184-j247

(b) Eigenvalues for Equation 25

$$\text{Stiffness ratio} = \frac{10410}{102.9} = 101$$

Table 3. The Eigenvalues of Jacobian Matrix For Three Equations Unconstrained System

7. Reduced-order MHD Model

At the initial state, i.e., time=0, the time derivatives for the three discretized conservation equations have been calculated. The normalized rate ρ_t/ρ for the mass conservation equation is about 70, the normalized rate U_t/U for the linear momentum equation is about 50, and the normalized rate T_t/T for the energy equation is about 10, so the mass conservation equation is comparatively faster than the momentum equation and the energy equation. This perhaps offers an opportunity to simplify the problem, in that, if the behavior of the density is assumed to be pseudo-steady, the conservation of mass partial differential equation may be reduced to an ordinary differential equation in the spatial independent variable only.

If this is done, equation (4) is reduced to

$$\frac{\partial(\rho UA)}{\partial x} = 0 \quad , \tag{32}$$

and equation (32) is expanded to

$$UA\frac{\partial \rho}{\partial x} + \rho A\frac{\partial U}{\partial x} + \rho U\frac{\partial A}{\partial x} = 0$$

or

$$\frac{\partial \rho}{\partial x} = -\frac{\rho}{U}\frac{\partial U}{\partial x} - \frac{\rho}{A}\frac{\partial A}{\partial x} \quad . \tag{33}$$

By substitution of equation (33) into equations (5) and (6), the MHD model reduces to a second-order model with the dependent variables velocity U and temperature T. The reduced-order model in matrix form is

$$\begin{bmatrix} 1 & 0 \\ 2U & c_p-R \end{bmatrix} \begin{bmatrix} U_t \\ T_t \end{bmatrix} = - \begin{bmatrix} U-RT/U & R \\ U^2 & c_pU \end{bmatrix} \begin{bmatrix} U_x \\ T_x \end{bmatrix} + \begin{bmatrix} \frac{RT}{A}\frac{A}{x} + (f_{JxB}\langle J_y\rangle\langle B\rangle)/\rho \\ (f_{J.E}\langle J_y\rangle\langle E_y\rangle + q_wP/A)/\rho \end{bmatrix} . \quad (34)$$

This is in the of form of equation (8).

Equation (33) and equation (34) are combined into a 1-ODE/2-PDE system. Elimination of the conservation of mass partial differential equation imposes a constraint on the solution of the remaining partial differential equations in the form of an implicit integral equation which must be solved iteratively at every grid point and every evaluation of the righthand sides of the discretized set of temporal ODEs. The process must continue until a stringent convergence criterion is met to prevent interaction between this implicit calculation and the error estimation or the Jacobian estimation by numerical first differences internal to LSODE.

If the resulting 1-ODE/2-PDE model is discretized in standard form, i.e., equation (9), and Pseudocharacteristic form, i.e., equation (25), the Jacobian maps are shown in Figure 7 and Figure 8 for sequential equations. The Jacobians are block banded plus lower triangular. Figure 9 and Figure 10 are Jacobian maps for equation (9) and equation (25) with the discretized equations grouped by grid point (interleaved) instead of by PDE origin (sequential).

The eigenvalues of the Jacobian matrices are listed in Table 4. It shows that the stiffness ratios of the reduced-order models are reduced by a factor of four for Method of Lines and a factor of nine for method of Pseudocharacteristics.

65 - 15 (standard form)

101 - 11 (pseudocharacteristic form)

and the number of ordinary differential equations is reduced.

```
               1111111111222
      1234567890123456789012
 1
 2    878        868
 3    6777        868
 4    66878        868
 5    666777        868
 6    6664878        868
 7    66644777        868
 8    666444777        868
 9    6664444676        868
10    66644444777        868
11    66644444788        888
12
13    868        868
14    6878        868
15    66868        868
16    665878        868
17    6653868        868
18    66534878        868
19    665343878        868
20    6654434878        868
21    66644343878        868
22    66644444888        899
```

Figure 7. Jacobian Map for Reduced-order Model in form of Equation (9) Sequential

```
               1111111111222
      1234567890123456789012
 1
 2    8887       7887
 3    67887      78787
 4    677887      78787
 5    6667887      78787
 6    66667887      78787
 7    666277887      78787
 8    6662277887      78787
 9    66622176887      78786
10    66622227877       7887
11    66622227887       7888
12
13    8887       8888
14    78787      88886
15    678787      88886
16    6678787      88886
17    66578787      88886
18    665278787      88886
19    6652278787      88886
20    66522178786      88886
21    66622117887       8888
22    66622117888       8999
```

Figure 8. Jacobian Map for Reduced-order Model in form of Equation (25) Sequential

```
             1111111111222
    1234567890123456789012
 1
 2
 3  887688
 4  886688
 5  6 787678
 6  6 887688
 7  6 6 887688
 8  6 6 886688
 9  6 6 6 787678
10  6 6 5 887688
11  6 6 6 4 887688
12  6 6 5 3 886688
13  6 6 6 4 4 787678
14  6 6 5 3 4 887688
15  6 6 6 4 4 4 787678
16  6 6 5 3 4 3 887688
17  6 6 6 4 4 4 4 687668
18  6 6 5 4 4 3 4 887688
19  6 6 6 4 4 4 4 4 787678
20  6 6 6 4 4 3 4 3 887588
21  6 6 6 4 4 4 4 4 788888
22  6 6 6 4 4 4 4 4 888989
```

Figure 9. Jacobian Map for Reduced-order Model in form of Equation (9) Interleaved

```
             1111111111222
    1234567890123456789012
 1
 2
 3  87888877
 4  88888878
 5  6778878877
 6  7888788876
 7  6 7778878877
 8  6 7888788876
 9  6 6 6778878877
10  6 6 7888788876
11  6 6 6 6778878877
12  6 6 5 7888788876
13  6 6 6 2 7778878877
14  6 6 5 2 7888788876
15  6 6 6 2 2 7778878877
16  6 6 5 2 2 7888788876
17  6 6 6 2 2 1 7768878876
18  6 6 5 2 2 1 7888788866
19  6 6 6 2 2 2 2 77887877
20  6 6 6 2 2 1 1 78888878
21  6 6 6 2 2 2 2 77888878
22  6 6 6 2 2 1 1 78898989
```

Figure 10. Jacobian Map for Reduced-order Model in form of Equation (25) Interleaved

(a)	(b)
-243+j7576	-3736+j8311
-243-j7576	-3736-j8311
-603+j6427	-2941+j7965
-603-j6427	-2941-j7965
-1155+j4758	-4457+j6052
-1155-j4758	-4457-j6052
-3650	-5161+j3560
-1654+j2674	-5161-j3560
-1654-j2674	-5354+j1074
-2615	-5354-j1074
-313+j2521	-1825+j3386
-313-j2521	-1825-j3386
-333+j1756	-1603+j2427
-333-j1756	-1603-j2427
-1320	-1213+j1462
-448	-1213-j1462
-444+j604	-526+j827
-444-j604	-526-j827
-381+j1138	-451+j197
-381-j1138	-451-j197
(a) Eigenvalues for Equation (9)	(b) Eigenvalues for Equation (25)
Stiffiness ratio $= \frac{3650}{242.5} = 15$	Stiffiness ratio $= \frac{5161}{450.5} = 11$

Table 4. The Eigenvalues of the Jacobian for Reduced-order Model

By transformation of equation (34) to the standard form of equation (9) and application of the Method of Lines to the reduced-order model, if upwind or biased upwind approximations are used to replace the spatial derivatives, the solutions are numerically unstable. If the centered three-point approximation is used to replace the spatial derivatives, the solution is stable but distorted as before.

The application of the method of Pseudocharacteristics to the reduced-order model follows the same process as for the three equation unconstrained MHD model, the Pseudocharacteristic form of equation (25) is obtained by finding the eigenvalues of matrix $\underline{A}$ in equation (9) and obtaining the transformation matrix $\underline{B}$ from equation (17). Matrix $\underline{B}$ is defined as

$$\underline{B} = \begin{bmatrix} B_{11} & 1 \\ B_{21} & 1 \end{bmatrix}$$

The Pseudocharacteristic form of the set of ordinary differential equations, equation (30), is

$$\begin{matrix} U_t \\ T_t \end{matrix} = -\begin{bmatrix} B_{11} & 1 \\ B_{21} & 1 \end{bmatrix}^{-1} \begin{bmatrix} \lambda_1 (B_{11} U_{x+} + T_{x+}) \\ \lambda_2 (B_{21} U_{x-} + T_{x-}) \end{bmatrix} + \begin{bmatrix} f_1 \\ f_2 \end{bmatrix} . \qquad (35)$$

Stable solutions of the reduced-order model can be obtained by use of higher-order biased upwind finite difference formulas to replace the spatial derivatives. The numerical results do not agree very well with the results of the three equation unconstrained model. It casts doubt on the pseudo-steady assumption. Besides the fact that the conservation of mass equation is not very much faster than the momentum and energy equations, there is a better way to determine if the system separates into different time-scale systems, see Anderson [12]. For a system of coupled linear first-order differential equations, i.e., $\dot{\underline{x}} = \underline{Ax}$, the n eigenvalues of matrix $\underline{A}$ can be separated according to absolute value into nonempty sets S and F. Set S contains n_1 nonzero eigenvalues and set F contains n_2 nonzero eigenvalues, where $n = n_1 + n_2$. A system parameter used to measure two-time-scale linear system separation is defined by

$$r = \frac{|S_{n1}|}{|f_1|} << 1 \quad .$$

where S_{n1} represents the largest absolute eigenvalue of set S and f_1 represents the smallest absolute eigenvalue of set F.

In the MHD model, the absolute eigenvalues are calculated from Table (3a) which represent the eigenvalues at steady state. They are

(1) 14840	(9) 4182
(2) 12706	(10) 3094
(3) 10310	(11) 1537
(4) 9680	(12) 1342
(5) 7310	(13) 1127
(6) 6246	(14) 760
(7) 6184	(15) 360
(8) 4841	(16) 573 .

These eigenvalues may be separated into two sets. It can be shown that the eigenvalues (11) to (16) come from the density equation. Let eigenvalues (11) to (16) belong to set S and the remainder belong to set F. The ratio r is 1537/3094=0.5. In this case r is not much less than 1, which indicates that the density equation was not of a sufficiently different time scale from the remainder of the model and therefore not a pseudo-steady phenomenon.

However, the steady state solutions do agree with those of the three equation model and there may be instances when the reduced-order model offers an economical means to obtain steady state solutions in comparison to use of the unconstrained model.

Also, for large system numerical simulation, the reduced order model is very useful if the problem is a multi-time-scale system.

8. Numerical Results

A 31 point grid and split boundary conditions were used to obtain the sample results shown in Figure 11 for mass density, Figure 12 for velocity and Figure 13 for temperature as three dimensional plots. The temperature and pressure were specified at the first, or leftmost, gridpoint, and the pressure was specified at the thirty-first, or right most, gridpoint. Direction of flow is from left to right. The disturbance is introduced by suddenly raising the pressure, or density, at the righthand end. This is unrealistically severe but it does introduce a prominent transient and permit demonstration of the reflective properties of the solution technique.

The same 31 point grid and split boundary conditions were used to obtain the sample results for the constrained reduced-order model shown in Figure 14. All the profiles are plotted under the same conditions. The three dimensional plots represent the transient responses of one meter of MHD channel when the upstream temperature and pressure are maintained at 2696.6 K and 422990. N/m^2. Profiles are plotted every 1 millisecond interval along the time coordinate t and every 0.033m interval along the spatial coordinate x. The second profiles along the x axis are the profiles at 1.0ms at which time the pressure at 1.0m was increased by 40000 N/m^2 resulting in an instantaneous increase in the density at 1,om. The third profiles along x axis occurred at 2.0 ms and began to show the propagation of the disturbance.

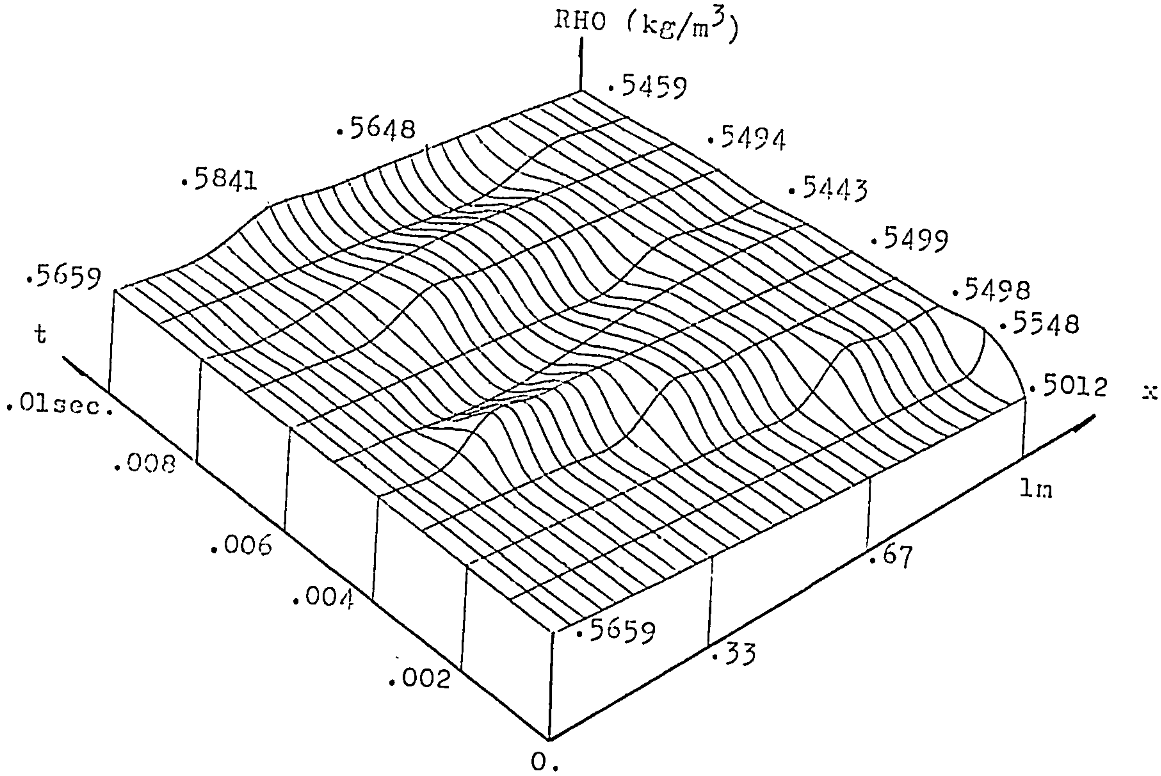

Figure 11. Density Variation Resulting from a Step Increase in Downstream Pressure.

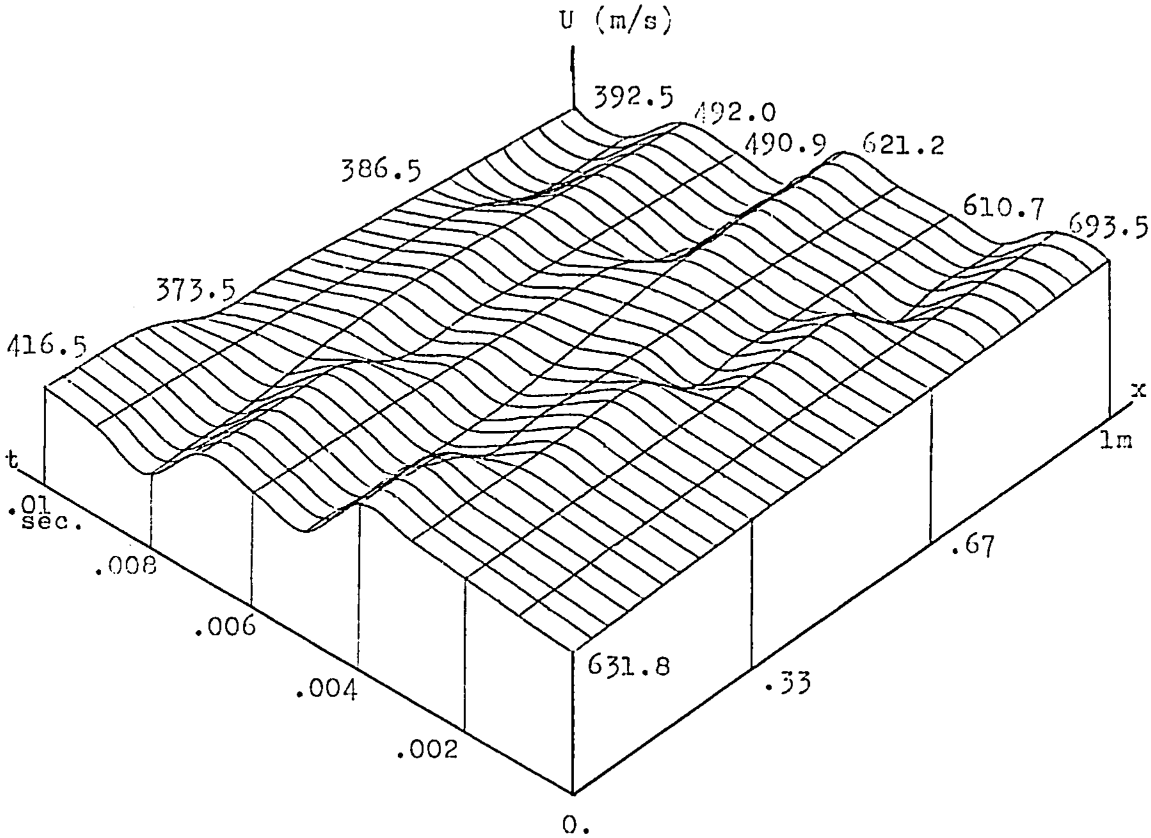

Figure 12. Velocity Variation Resulting from a Step Increase in Downstream Pressure

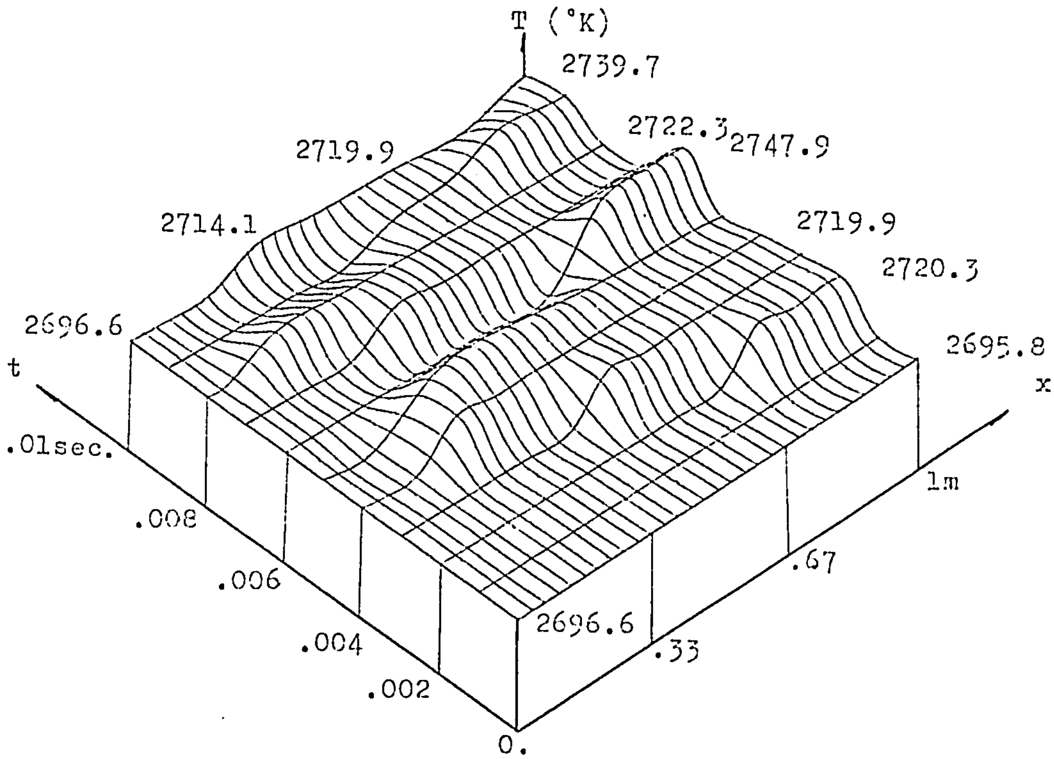

Figure 13. Temperature Variation Resulting from a Step Increase in Downstream Pressure

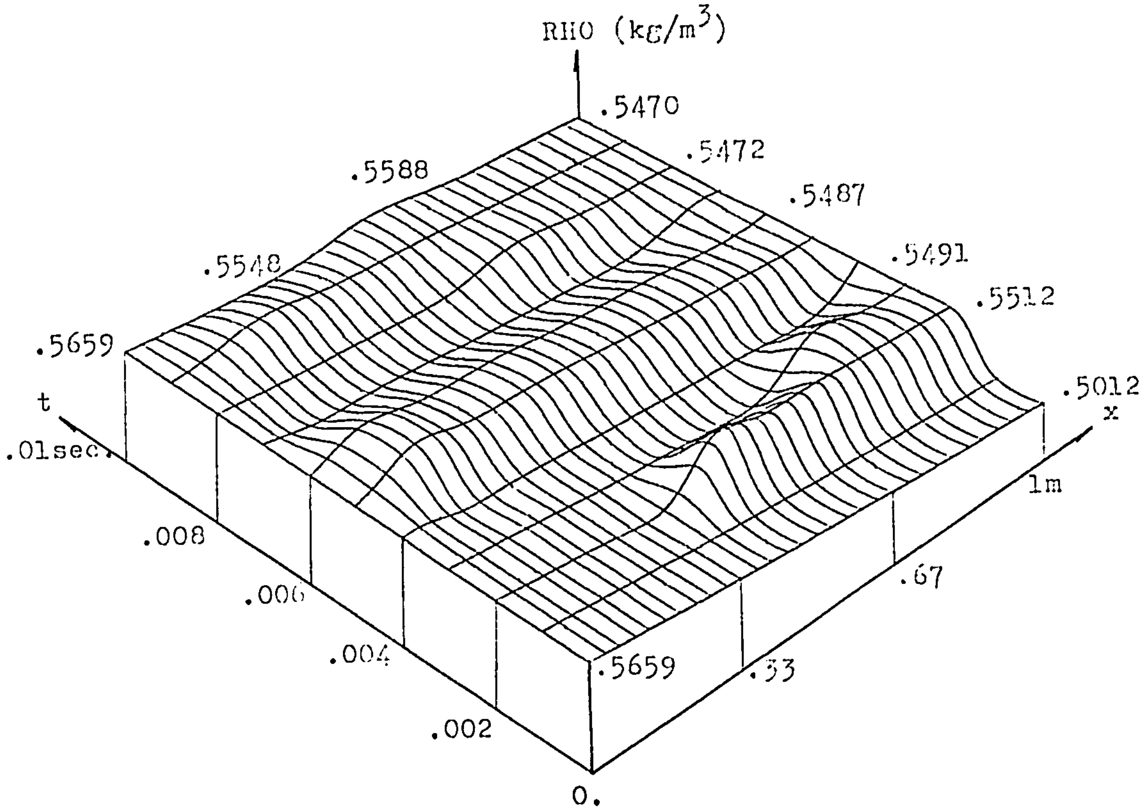

Figure 14. Reduced Order Model Transient Response for Density Variation

9. Conclusion

This work presents an example of the Pseudocharacteristic method described by Carver [1].

The method of Pseudocharacteristics for hyperbolic PDEs is a combination of the method of characteristics on a fixed grid and the Numerical Method of Lines. It permits flexible application of a wide variety of spatial derivative replacement algorithms. The spatial derivative replacements used must be apporpriately biased according to the signs of associated eigenvalues because of the directional nature of hyperbolic equations. It permits application of a powerful general-purpose integration software package which has many options and diagonostic tools. It is convenient to control the integrator performance. Therefore, more accurate and less diffused numerical results can be achieved by the method of Pseudocharcteristics.

The MHD channel simulation provided a set of nonlinear, nonconservative PDEs which were solved successfully and rather straightforwardly by the method of Pseudocharacteristics after a standard Method of Lines formulation had failed to produce credible results.

References

1. Carver, M.B., "Pseudo-Characteristic Method of Lines Solution of First-Order Hyperbolic Equation Systems", Advances in Computer Method for Partial Differential Equations-III, Proceedings of the Third IMACS International Symposium on Computer Methods for Partial Differential Equations held at Lehigh U., Bethlehem, PA, June 20-22, 1979, R.Vichnevetsky and R.S. Stepleman, editors, pp 227-232.

2. Oliver, D.A., R.D. Crouse, C.D. Maxwell and S.T.Demetriades, Transient Processes in Large Magnetohydrodynamic Generator Flow-trains", The International Conference on MHD Electrical Power Generation, June, 1980.

3. Johnson, S.H. and A.C.Hindmarsh, "Numerical Dynamic Simulation of Solid-Fluid Reactions in Isothermal Porous Spheres", in preparation.

4. Dissinger, G.R., W.E.Schiesser and S.H.Johnson, "Large Scale Dynamic Process Simulation Experience: Effect of Jacobian Structure on Integrator Performance", Advances in Computer Technology - 1980 Vol.1, ASME.

5. Hindmarsh, A.C., "LSODE and LSODI, Two New Initial Value Ordinary Differential Equation Solvers", ACM SIGNUM Newsletter, Vol. 15, No. 4, December 1980, pp. 10-11.

6. Courant, R., E.Isaacson and M.Rees, "On the Solution of Nonlinear Hyperbolic Differential Equations by Finite Differences", Comm. on Pure and Applied Math., Vol. V, 1952, pp.243-255.

7. Hancox, W.T. and S.Banerjee, "Numerical Standards for Flow-Boiling Analysis", Nuclear Science and Engineering, Vol.64, 1977, pp.106-123.

8. Hancox, W.T. and B.H.Mcdonald, "Finite Difference Algorithms to Solve the One-Dimensional Flow-Boiling Equations", Invited paper at the ANS/ASME International Topical Meeting on Nuclear Reactor Thermal-Hydraulics, Saratoga Springs, NY, October, 1980.

9. Ferch, R.L., "Method of Characteristics Solutions for Nonequilibrium Transient Flow Boiling", Int. J. of Multiphase Flow, Vol.5, No.4, 1979, pp.265-279.

10. Wang,Y-Z and S.H. Johnson, "Application of the Pseodo-Characteristic Numerical Method of Lines", Proceedings of the 10th IMACS World Congress on System Scientific Computation held at Montreal, Canada, Augest 8-13, 1982, Vol.1, pp 146-148.

11. Kolev, N.P. and E.A.Katkovsky, "A Comparative Study of the Pseudocharacteristic and Two-Step LW Method in Flow-Boiling Problems", Advances in Computer Methods for Partial Differential Equations-IV, Proceedings of the Fourth IMACS International Sympoisum on Computer Methods for Partial Differential Equations held at Lehigh U., Bethlehem, PA, June 30-July 2, 1981, R.Vichnevetsky and R.S.Stepleman, editors, pp.391-398.

12. Anderson,L., "Decoupling of Two-Time-Scale Linear System", Joint Automatic Control Conference Vol.4, October 18-20,1978, Philadelphla, PA.

13. Gyarmati, Istvan, Non-Equilibrium Thermodynamics: Field Theory and Variational Principles, Springer-Verlag, 1970.

Nomenclature

t = Time (s)

ρ = Mass density (kg/m^3)

U = Axial velocity (m/s)

T = Temperature (°K)

A = Local duct cross-sectional area (m^2)

P = Local perimeter (m)

q_w = Average heat flux (KJ/s)

c_p = Heat capacity of gas (Kcal/kg°K)

R = Gas constant (KJ/kg°K)

p = Pressure (N/m^2)

ε = Internal energy (KJ/kg)

h_o = Stagnation enthalpy (KJ/kg)

τ_w = Average wall shear stress over the cross-section (N/m^2)

$f_{JxB}\langle J_y\rangle\langle B\rangle$ = Lorentz force in the axial direction (N/m^3)

$f_{J.E}\langle J_y\rangle\langle E_y\rangle$ = Lorentz power (W/m^3)

Vita

Yi-Zun Wang was born on June 12, 1949, in Peking, China. She entered the Girls High School of Peking University of Teacher Training in 1962 and graduated in 1968.

In September 1973, she entered the Peking University of Iron and Steel Technology and graduated in December 1976. Subsequently, she worked in the Department of Mechanical Engineering of the Peking University of Iron and Steel Technology as a research and teaching assistant.

In August 1979, she entered the Department of Mechanical Engineering and Mechanics, Lehigh University.